Journal of Techniques, ISSN: 2708-8383, Vol. 6, No. 1, 2024, Pages 45-51
DOI: https://doi.org/10.51173/jt.v6i1.2114

JOURNAL OF TECHNIQUES

Journal homepage: http://journal.mtu.edu.iq

RESEARCH ARTICLE - MECHANICAL ENGINEERING

# Influence of Welding Parameters on Mechanical Properties and Microstructure of Similar Low-Carbon Steel AISI 1005 Welding by Resistance Spot Welding

**Osamah Sabah Barrak[1*], Slim Ben-Elechi[1], Sami Chatti[1]**

[1]National Engineering School of Monastir, University of Monastir, LGM, ENIM, Avenue Ibn-Eljazzar, 5019 Monastir, Tunisia

[*] Corresponding author E-mail: usamah.barrak@yahoo.com

**Article Info.**

*Article history:*

Received
28 October 2023

Accepted
08 December 2023

Publishing
31 March 2024

**Abstract**

Resistance spot welding (RSW) was used to fabricate similar joints of low-carbon steel AISI 1005 in a lap joint design. The welding current, squeeze time, welding time, and hold time, which affect resistance spot welding, were evaluated. A tensile-shear force fracture test was used to assess the mechanical properties using a universal tensile testing machine. The microstructure of the fusion zone was examined using a scanning electron microscope (SEM). According to the data, the shear strength values increased as the welding current increased. Additionally, it was shown that most failures occurred closer to the fusion zone (FZ). The primary cause is the crystal lattice's strained distortion, which weakens the nearby region of the fusion zone.



Publisher: Middle Technical University

**Keywords**: Resistance Spot Welding (RSW); Low-Carbon Steel; AISI 1005.

## 1. Introduction

In recent times, the automotive industries have employed new materials to enhance the safety of vehicle components at a low cost; by increasing the material's properties, such as a high strength-to-weight ratio and enhancing performance, these new materials help produce cars more fuel efficiently [1-3]. The main objective of choosing new materials is to resolve present challenges before manufacturing. Low-carbon steel is a highly desired category in metallurgical steel as it can be easily welded to form a combination of martensite and ferrite phases [4, 5]. For automotive applications, low-carbon steel is compatible with materials that have good elongation and ductility, which is always necessary. Additionally, its strength, toughness for crashworthiness, and enhanced efficiency of the vehicle body due to weight reduction make it attractive to the automotive industry [6].

The most common method of joining steel sheets, especially in the automobile industry, is resistance spot welding (RSW). This technique has the advantages of simplicity, low cost, rapidity (short process time), and automation possibilities. The joining of low-carbon steel sheets is attractive because the mechanical characteristics of spot welds are essential. A significant factor is the difference in low-carbon steel characteristics during the spot-welding process [7, 8]. RSW significantly affects how automotive bodies are assembled. In order to increase the joint integrity of the welding used in chassis assembly, it is also essential to increase the dependability of metal joining. The material properties of an automobile body are not the only factors that affect its performance. It also depends on the quality of the joint, which is a representation of metallurgical deformation on welding heat generated; compared to other welding methods, it allows for a variety of complex microstructures at an essential cooling rate [9, 10].

The mechanical characteristics and welding behaviour of low-carbon have been extensively studied [11, 12]. In order to determine the maximum strength of the weld spot, Shen et al. analyse the resistance spot welded dual phase steels' tensile shear test behaviour. They also characterise the different forms of loads and display the deformation mode on the weld joint during the crash event [13]. In addition to peak load, resistance spot welds' ability to absorb energy should also be considered when studying the mechanical behaviour of RSWs, according to Zuniga [14] and Zhou et al. [15]. Zhou et al. [15] established a relationship between the peak load and energy absorption of spot welds by computer simulation utilising the design of the experiments (DOE) method, which included the electrode indentation depth, HAZ size, and weld size.

The present investigation examined the shearing force of RSW joints with varying welding parameters, including welding current, squeeze time, welding time, and hold time. The low-carbon steel AISI 1005 was joined using the RSW technique.

| **Nomenclature & Symbols** | | | |
|---|---|---|---|
| AISI | American Iron and Steel Institute | RSW | Resistance Spot Welding |
| FZ | Fusion Zone | DOE | Design of Experimental |
| HAZ | Heat-Affected Zone | SEM | Scanning Electron Microscope |
| WN | Weld Nugget | kA | Kilo Ampere |

The mechanical characteristics (shearing force) of RSW joints were assessed using a scanning electron microscope (SEM). Furthermore, a design of experiments (DOE) was employed to assess the impact of welding parameters on the sheer force of RSW joints and to analyze the mechanical characteristics of RSW joints under various welding conditions.

## 2. Experimental Setup

The material used for this investigation is 1 mm thick low-carbon steel, AISI 1005. The elemental composition of this material is present in Table 1; the mechanical properties of AISI 1005 are represented in Table 2.

Table 1. Chemical Composition of AISI 1005

| **Element wt %** | **C%** | **Ni%** | **P%** | **S%** | **Cr%** | **Mn%** | **Cu%** | **Fe%** |
|---|---|---|---|---|---|---|---|---|
| AISI 1005 | 0.08 | 0.024 | 0.01 | 0.026 | 0.04 | 0.38 | 0.048 | Bal. |

Table 2. Mechanical properties of AISI 1005

| **Material Property** | **Yield Strength (MPa)** | **Tensile Strength (MPa)** | **Elongation (%)** |
|---|---|---|---|
| AISI 1005 | 185 | 326 | 34 |

The welding experiments were performed on AISI 1005 under the welding conditions using resistance spot welding equipment shown in Fig. 1. The welding current, squeeze time, welding time, and hold time are the four factors with four levels that make up the welding parameters used in this study.

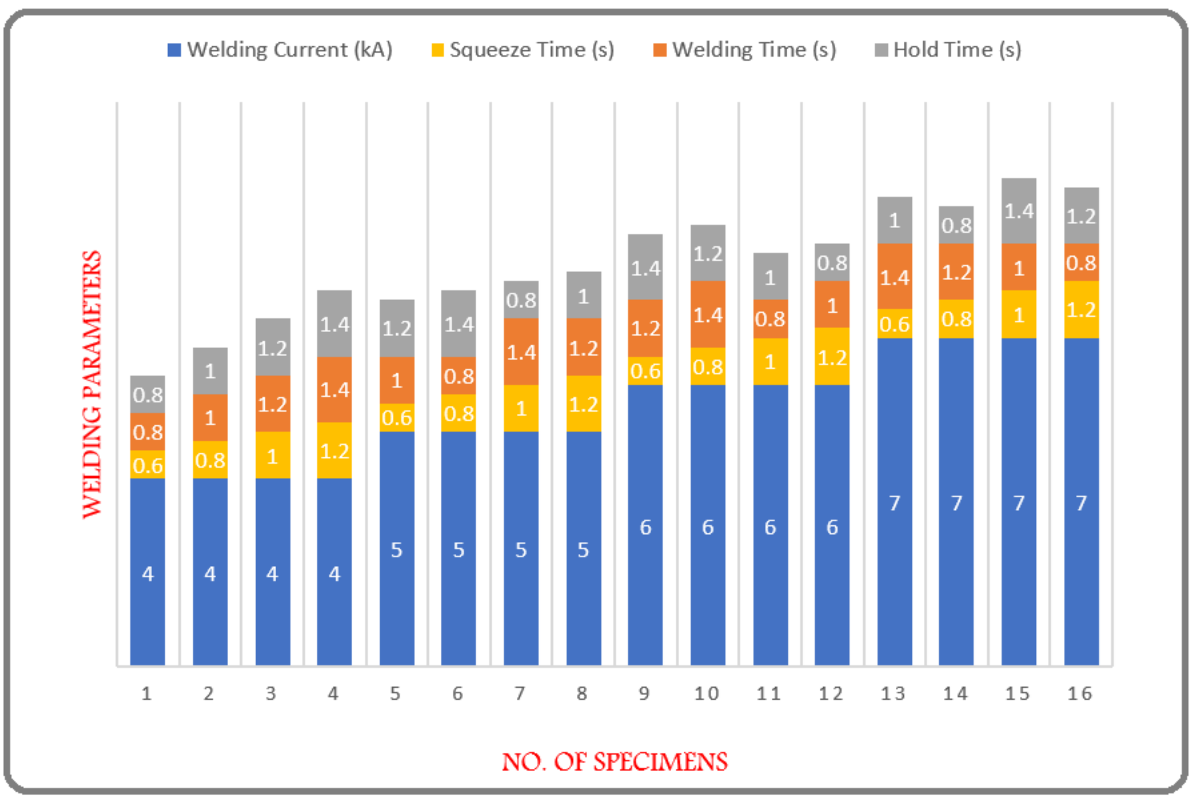


Fig. 1. Welding Parameters

The material dimensions to be welded, AISI 1005 steel, described in Fig. 2, follow the ANSI/AWS C1.1M/C1.1:2012 standards [16]. The shear-tensile force of resistance spot-welded AISI 1005 steel joints was investigated using the tensile shear fracture test utilizing universal tensile testing equipment. As illustrated in Fig. 3, the semi-automatic tensile testing machine has a maximum capacity of approximately 50 KN. Fig. 4 depicts the defect-free resistance spot welded joint and demonstrates the excellent nugget formation among the different AISI 1005 joint levels.

The microstructural characteristics obtained from the spot-welded joint's cross-section were examined using a scanning electron microscope (SEM). The sample was polished employing belt grinders and disk polishing devices with several grades of silicon carbide abrasive paper. With the use of finely micron-level alumina powder and diamond paste, excellent polishing has been accomplished.

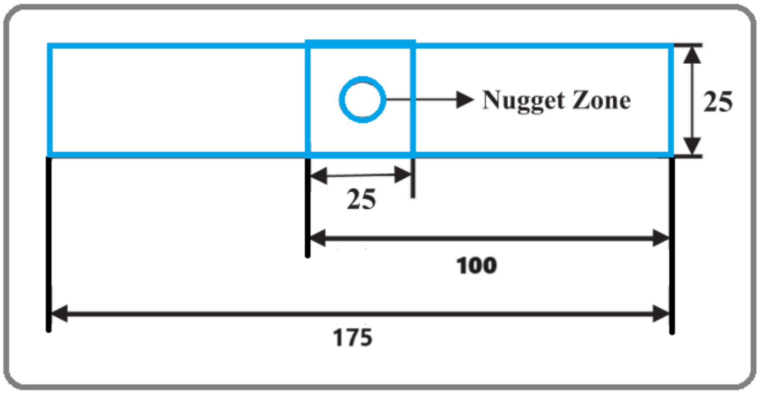


Fig. 2. Test specimen dimensions (in mm)

Fig. 3. Tensile Test

Fig. 4. Welded Specimen

## 3. Results and Discussion

### *3.1. Scanning Electron Microscope (SEM)*

The nugget increases with the welding current, while the formation's lap joints have a more comprehensive range. The influence of welding parameters on different macrographs is displayed in Fig. 4, which shows variations in the weldment's nugget development. The nugget increases with the welding current, while the formation's lap joints have a more comprehensive range. Increasing the welding current even further leads to pull-out failure and compromises the integrity of the joint. A macro-level defect-free joint with improved nugget formation is achieved with a welding current level of 7 kA.

Fig. 5 shows the microstructure of the Nugget Zone. During the welding process, a fusion zone (FZ) or weld nugget (WN) melts and resolidifies. The weld nugget shape exhibits an asymmetry in its microstructure. The primary characteristic determining the mechanical performance of the spot welds is the size of the weld nugget. Fig. 5 depicts a typical cross-section profile of a spot weld. The resulting microstructure is primarily ferrite–martensite and consists of martensite, upper binaite, and Widmanstätten (side plate) ferrite.

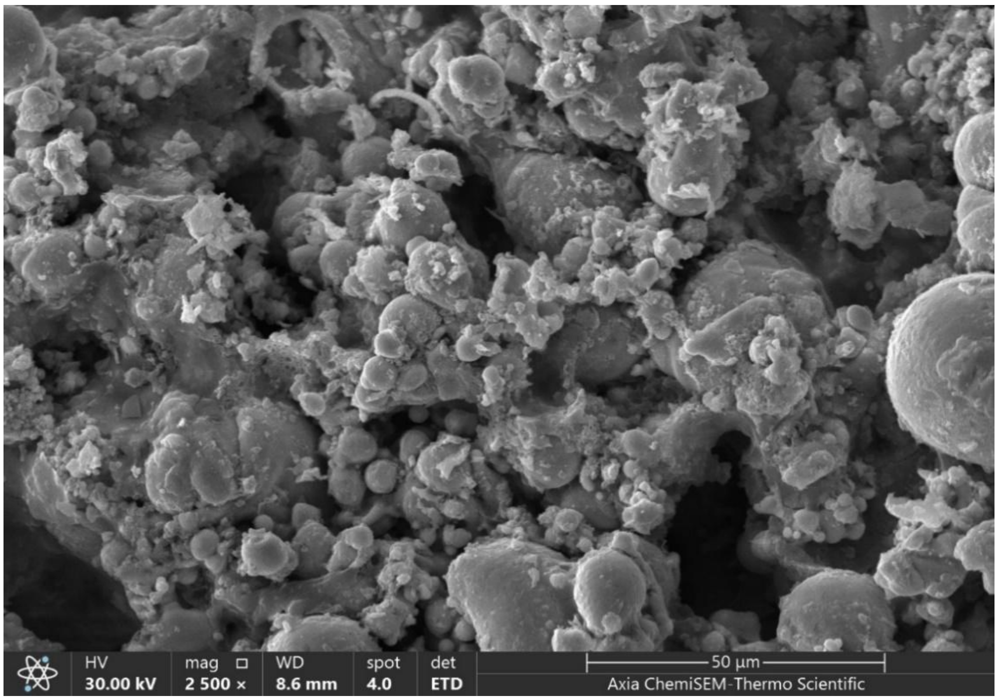


Fig. 5. SEM of resistance spot-welded AISI 1005

### *3.2. Mechanical properties of AISI 1005 lap joint*

Fig. 6 shows specimens after the tensile-shear test. Pull-out is the failure mode, and the fracture started around the weld nugget at an outside edge point. The graph of tensile-shear force vs. number of specimens is displayed in Fig. 7.

In comparison to other welding parameters, the highest tensile shear fracture force value that was observed was around 5.542 kN at (7 kA welding current, 0.8s Squeeze Time, 1.2s Welding Time, 0.8s Hold Time). The nugget area increases with increased welding current, which occurs at different levels. The heat-affected zone's (HAZ) interfacial region, which has already been developed with the assistance of microstructure, is where most tensile failure occurs. The formation of tempered martensite in the HAZ, which exhibits properties of a more failure-brittle nature, and the rate of cooling are the categories caused by these fracture modes [17, 18].

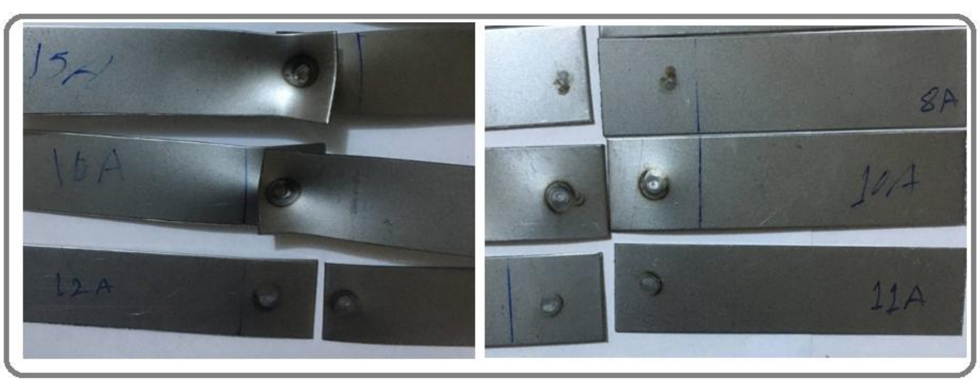

Fig. 6. After the tensile-shear test

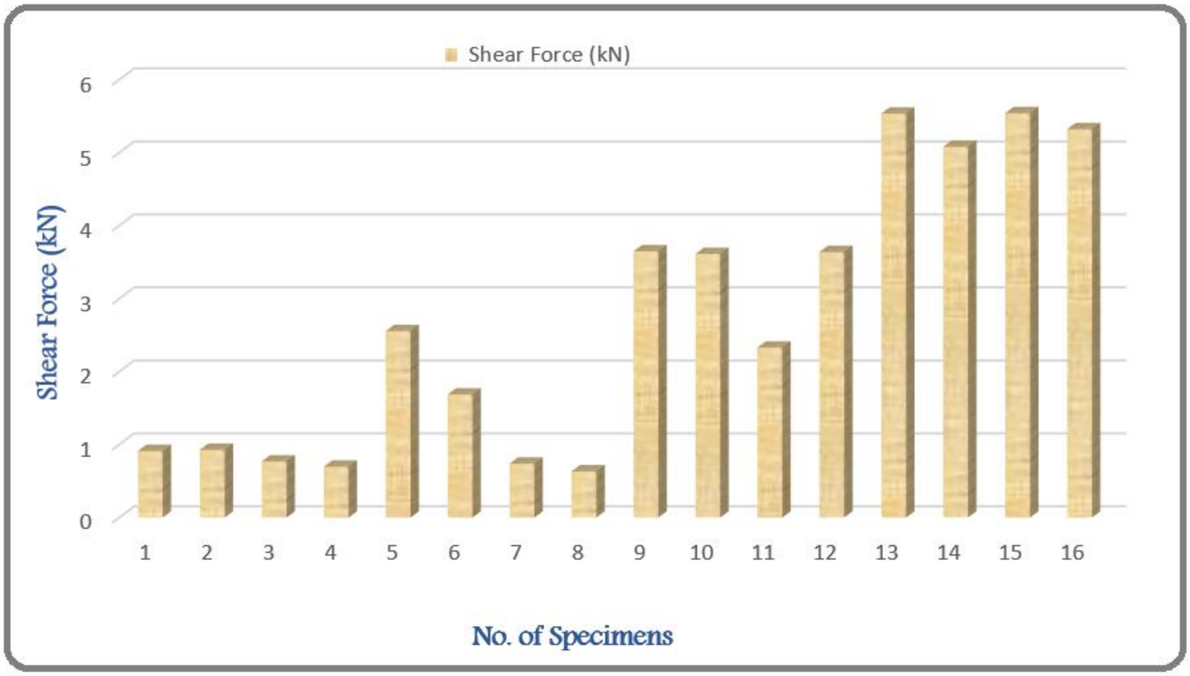


Fig. 7. Shear force results of AISI 1005

Using the Minitab 17 program, the tensile shear force was analysed by applying the Taguchi evaluation approach to determine the best level of welding parameters and investigate the influence of the welding parameters on the joint's strength. This approach improves the shear force. Fig. 8 illustrates how the joint force is affected by the welding parameters (welding current, squeeze time, welding time, and hold time). The joint shear force will rise as the welding current increases. At the same time, the other welding parameters have an alternating effect on the joint shear force. Furthermore, Fig. 9 demonstrates that the welding current significantly influences the joint tensile shear force more than the other welding parameters.

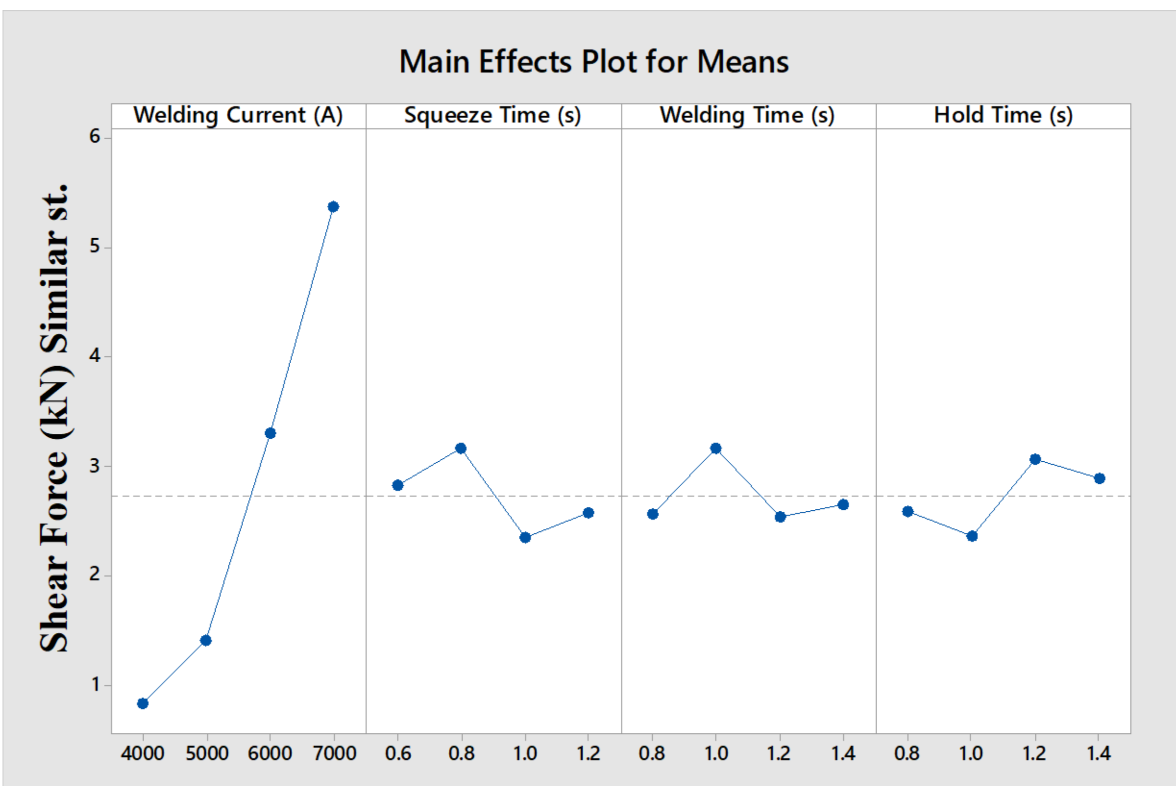


Fig. 8. Main effect plot of AISI 1005

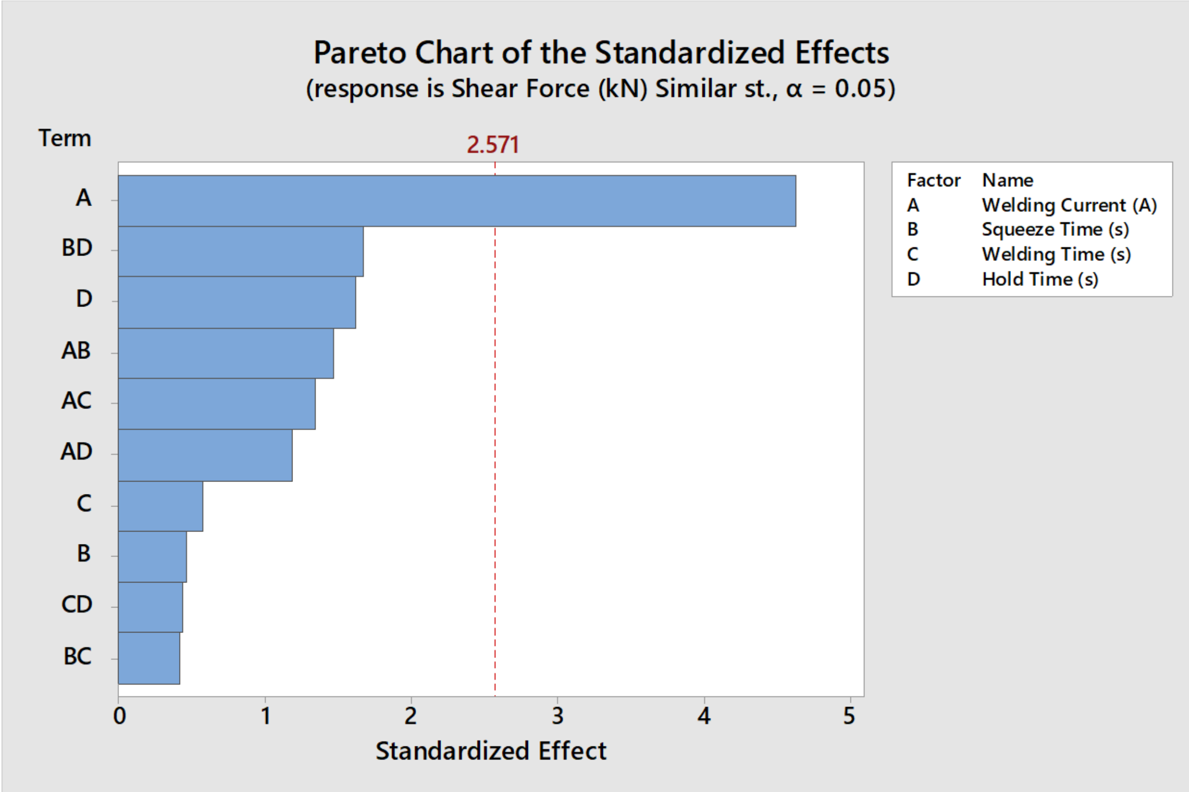


Fig. 9. Pareto chart of AISI 1005

## 4. Conclusion

The welding parameter most affected by the AISI 1005 steel RSW technique is the welding current. When the welding current increases, the depth of the nugget zone grows, which increases the weld shear force. The microstructure of the fusion zone consists of martensite, upper bainite, and Widmanstätten (side plate) ferrite. The interfacial zone's tempered martensite, which is closer to the HAZ, is the cause of the weld failure. The fracture mode illustrated interfacial failure and pull-out failure.

## Acknowledgement

We would like to thank the head of the Department of Technical Applied Mechanical Engineering and all the department's teaching staff for their assistance.

## References

[1] Zhang, P., et al. "Effects of welding parameters on mechanical properties and microstructure of resistance spot welded DP600 joints." Science and Technology of Welding and Joining, vol. 16, no. 7, 567-574, 2011, https://doi.org/10.1179/136217110x12813393169732.
[2] Sun, H. T., et al. "Effect of variable electrode force on weld quality in resistance spot welding." Science and Technology of Welding and Joining, vol. 12, no. 8, 718-724, 2007, https://doi.org/10.1179/174329307x251862.
[3] Osamah Sabah Barrak, Osamah Fattah Taresh, Mahmood Mohammed Hamzah, and Rusul Ahmed Shakir, “An Investigation of Joining Polyamide (PA) to Stainless Steel AISI 316L by Hot Press Process”, JT, vol. 5, no. 1, pp. 114–121, Apr. 2023, https://doi.org/10.51173/jt.v5i1.1280.
[4] Zhao, D. W., et al. "Effects of electrode force on microstructure and mechanical behavior of the resistance spot welded DP600 joint." Materials & Design, vol. 50, 72-77, 2013, https://doi.org/10.1016/j.matdes.2013.02.016.
[5] Hassoni, S. M., Barrak, O. S., Ismail, M. I., & Hussein, S. K. "Effect of Welding Parameters of Resistance Spot Welding on Mechanical Properties and Corrosion Resistance of 316L." Materials Research, vol. 25, 2022, https://doi.org/10.1590/1980-5373-MR-2021-0117.
[6] Zhou, Kang, and Lilong Cai. "Study on effect of electrode force on resistance spot welding process." Journal of applied physics, vol. 116, no. 8, 2014, https://doi.org/10.1063/1.4893968084902.
[7] Khodabakhshi, F., M. Kazeminezhad, and A. H. Kokabi. "Mechanical properties and microstructure of resistance spot welded severely deformed low carbon steel." Materials Science and Engineering: A, vol. 529, 237-245, 2011, https://doi.org/10.1016/j.msea.2011.09.023.
[8] Ridha, M. H., Saad, M. L., Abdullah, I. T., Barrak, O. S., Hussein, S. K., & Hussein, A. K. "Joining of Carbon Steel AISI 1006 to Aluminum Alloy AA6061-T6 Via Friction Spot Joining Technique." International Journal of Applied Mechanics and Engineering, vol. 27, no. 4, 1-12, 2022, https://doi.org/10.2478/ijame-2022-0046.
[9] Wan, Xiaodong, Yuanxun Wang, and Peng Zhang. "Effects of welding schedules on resistance spot welding of DP600 steel." ISIJ International, vol. 54, no. 10, 2375-2379, 2014, https://doi.org/10.2355/isijinternational.54.2375.

[10] Sivaraj, P., Seeman, M., Kanagarajan, D., & Seetharaman, R. "Influence of welding parameter on mechanical properties and microstructural features of resistance spot welded dual phase steel sheets joint." Materials Today: Proceedings, vol. 22, 558-562, 2020, https://doi.org/10.1016/j.matpr.2019.08.201.
[11] Pouranvari, M., Abedi, A., Marashi, P., & Goodarzi, M. "Effect of expulsion on peak load and energy absorption of low carbon steel resistance spot welds." Science and Technology of Welding and Joining, vol. 13, no. 1, 39-43, 2008, https://doi.org/10.1179/174329307X249342.
[12] Pouranvari, M., Mousavizadeh, S. M., Marashi, S. P. H., Goodarzi, M., & Ghorbani, M. "Influence of fusion zone size and failure mode on mechanical performance of dissimilar resistance spot welds of AISI 1008 low carbon steel and DP600 advanced high strength steel." Materials & Design, vol. 32, no. 3, 1390-1398, 2011, https://doi.org/10.1016/j.matdes.2010.09.010.
[13] Shen, Jie, Yan Song Zhang, and xinmin Lai. "Effect of electrode force on expulsion in resistance spot welding with initial gap." Materials Science Forum, Vol. 675, Trans Tech Publications Ltd, 2011, https://doi.org/10.4028/www.scientific.net/msf.675-677.79.
[14] Zuniga, Steven Matthew. Predicting overload pull-out failures in resistance spot welded joints. Stanford University, 1994, https://www.proquest.com/openview/eb25c140d8ab600f1429e3ce1ffbe483/1?pq-origsite=gscholar&cbl=18750&diss=y.
[15] Zhou, M., H. Zhang, and S. J. Hu. "Relationships between quality and attributes of spot welds." Welding Journal-New York-, vol. 82, no. 4, 72-77, 2003.
[16] ANSI/AWS C1.1M/C1.1:2012, Recommended Practices for Resistance Welding, American Welding Society.
[17] Rajarajan, C., P. Sivaraj, and V. Balasubramanian. "Microstructural characteristics and load carrying capability of resistance spot welded dual phase (DP800) steel joints." Journal of Advanced Microscopy Research, vol. 13 no. 2, 198-203, 2018, https://doi.org/10.1166/jamr.2018.1379.
[18] Baltazar Hernandez, V. H., Panda, S. K., Okita, Y., & Zhou, N. Y. "A study on heat affected zone softening in resistance spot welded dual phase steel by nanoindentation." Journal of Materials Science, vol. 45, 1638-1647, 2010, https://doi.org/10.1007/s10853-009-4141-0.